CNU Journal of Higher Education
Volume 14 (2020), p 52-58

Superdiffusive Fractional Brownian Motion Memory of Annual Mean Global Temperature Anomaly

Karl Patrick S. Casas, Allan Roy B. Elnar and Gibson T. Maglasang
Cebu Normal University, The Philippines

Date Submitted: Ocotber 20, 2018
Date Revised: June 30, 2020

Originality: 85%
Plagiarism Detection: Passed

ABSTRACT

The NASA's GISTEMP Team temperature anomaly data from year 1880-2015 has undergone two different data treatments: 5-year moving average and second-generation data. Together with the untreated data, the log-log plot of mean square displacement (MSD) of temperature anomaly versus time was derived. Since it showed a linear response, fractional Brownian motion (fBM), which was derived using white noise analysis was shown. The fBM with Hurst exponent, $H = 1$ was then used as a fit to the MSD of temperature anomaly which implied super-diffusion. It must be pointed out that the upper bound of the H index is the condition necessary for the chosen memory function rendering the best fit to the temperature anomaly. Considering that global temperature follows a natural cycle when unperturbed, this anomalous behavior can be attributed to a driving *force* in the time evolution of the temperature anomaly. These 'forces' may be attributed to both the natural heating cycle in the Earth's surface and human activities particularly on technological changes and innovations which already begun even before the 1880s.

Keywords: *temperature anomaly, white noise analysis, mean square displacement, fractional Brownian motion, Hurst exponent*

INTRODUCTION

Greenhouse effect is a natural occurrence that maintains the Earth's average temperature. Without it, temperatures with be much lower compared today and the existence of life would not be possible. This is possible because of greenhouse gases that occur naturally: Carbon dioxide, methane, water vapor and nitrous oxide (Global Climate change, 2013). Nonetheless, the increase of greenhouse gases increases the greenhouse effect, which thereby increases the mean global temperatures as well as changes in precipitation patterns (Enzler, 2013). As a result, a net climate change will occur when there are changes in weather patterns in an area over a long period of time. These gradual changes in climate allow plants, animals and microorganisms to evolve and adapt to the new temperature of the environment (Global Climate change, 2013).

However, since the start of the first decade of the 21st century, the change is rapidly occurring which is the real threat of climate change. Since 1900, global temperatures have increased by 0.8 C. Aside from that, more evidences suggest that the mean global temperature increases at a rate of 0.4 F each decade (Global Climate change, 2013). The temperature, as one of the influencing parameters to changes in weather patterns, may be treated as a stochastic variable that may not seem to exhibit random pattern but rather a behavior with a memory of its past. Given that, a memory function may be extracted from the time series data of temperature anomaly. This may then be used to predict future trends of the increases of the surface temperature and for future mitigation and policy development.

Temperature Anomaly Time Series Data

Temperature anomaly is the difference from an *average* or *baseline* temperature, which is computed by averaging at least 30 years of temperature data. In the context of climate change, it is a more important term than the absolute temperature. This is because of the presence of some factors that may lead to problems when stations are added, removed, or missing from the monitoring network [Stock, 2015]. Some of these factors include station location or elevation that will have an influence on the temperature. Aside from that, some regions have fewer stations for the measurement of temperature, e.g., Sahara Desert. By using temperature anomaly instead, this effect is less critical (Stock, 2015; Hansen, 2016).

The temperature anomaly is used as a diagnostic tool to give scientist a big picture overview since it is a global scale data. In fact, this data is used for the analyses of global surface temperature change by several groups such as the NASA Goddard Institute for Space Studies, the NOAA National Climatic Data Center (NCDC), and a joint effort of the UK Met Office Hadley Centre and the University of East Anglia Climatic Research Unit (HadCRUT) (Hansen, 2010).

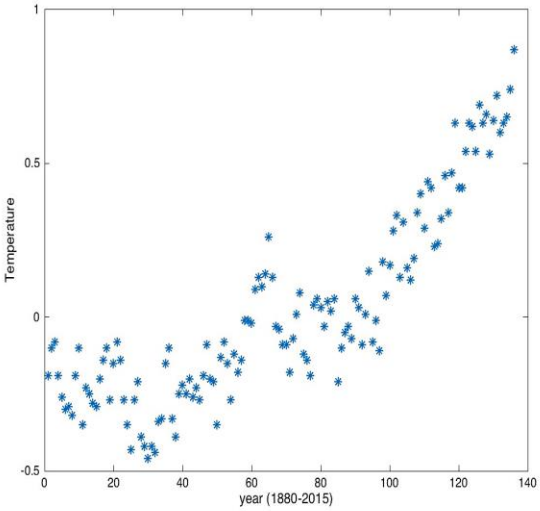

Figure 1. Plot of Temperature Anomaly from 1880 – 2015. A positive anomaly indicates that the observed temperature was warmer than the baseline. On the other hand, a negative anomaly indicates that the observed temperature was cooler than the baseline.

The annual global temperature anomaly data (GISTEMP Team, 2021; Lenssen et al., 2019) are available from the year 1880 up to 2015. This is shown in Figure 1. A positive anomaly signifies that the observed temperature was warmer than the baseline. On the other hand, a negative anomaly indicates that the observed temperature was cooler than the baseline temperature.

The data is subjected to different data treatment such as the second-generation data and moving average. To get the second-generation data, the temperature anomaly is fitted with a polynomial with n-degree using Matlab software. The polynomial fit that gives the highest chi-square is the degree 4. The temperature anomaly data points are then subtracted by the poly-4 fit, which generates the second-generation data. This is shown in Figure 2.

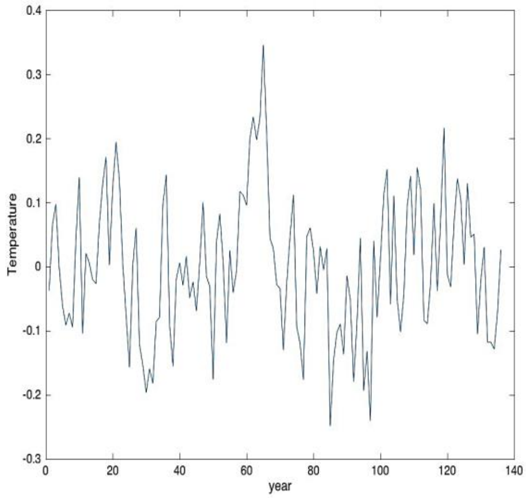

Figure 2. Plot of second-generation data derived from the Temperature Anomaly being subtracted by the poly-4 fit.

The mean square displacement of the temperature anomaly, which is the deviation from the mean, was also derived. This is done for the three different data sets (untreated, moving average and second-generation data). This is shown in Figure 3. We will then look at the memory function embedded in each data set, which will be discussed in the next two sections.

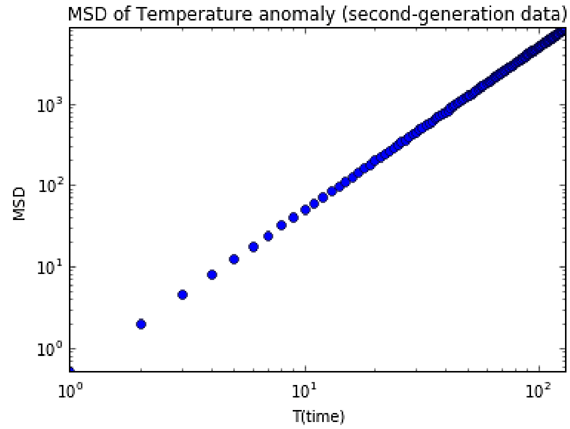

a

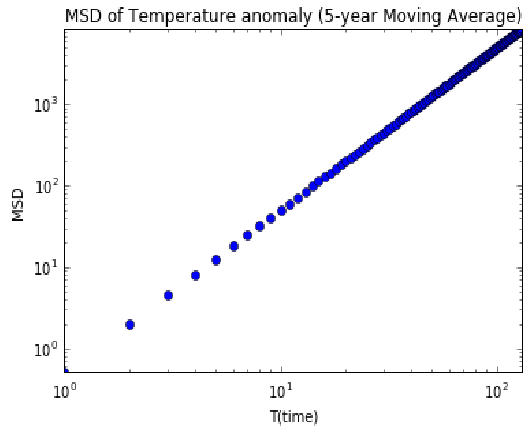

b

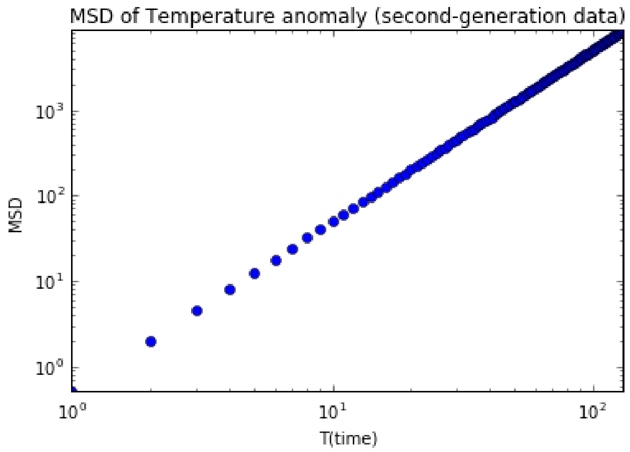

c

Figure 3. log-log MSD plots of the (a) untreated Temperature Anomaly, (b) Temperature anomaly in 5-year moving average and (c) Second-generation Temperature anomaly

White Noise Analysis

A stochastic random variable *x(t)* with no memory of its past can be written as the sum of its initial point x_0 and some Wiener process *B(t)* (Bernido & Carpio-Bernido, 2012),

$$x(t) = x_0 + B(t), \tag{1}$$

where $B(t) = \int \omega(t)dt$, where $\omega(t)$ is a random white noise variable. It is important to note in Equation (1) that the initial point is fixed at x_0 and the endpoint could be anywhere. A mathematical technique to deal with this dilemma is the use of a delta function, which can be written as $\delta(x(T) - x_T)$. One can then find the probability density function as the integral of the delta function over the gaussian white noise measure $d\mu_\omega$ (Bernido & Carpio-Bernido, 2012)

$$P(x_T, T; x_0, 0) = \int \delta(x(T) - x_T)\, d\mu_\omega, \tag{2}$$

However, several natural phenomena do not seem to fit randomness behavior as given by the Brownian motion in Eq. (1). Thus, to extend the applicability to a more dynamic evolution of real-world phenomena, a memory function $f(T-t)$ is added to the menu to allow the path $x(t)$ to have a memory of its past. The parametrization of the path will now be written as (Bernido and Carpio-Bernido, 2015)

$$x(T) = x_0 + \int_o^T f(T-t)h(t)\,\omega(t)dt, \tag{3}$$

Using Eq (2), the probability density function can then be written as

$$P(x_T, T; x_0, 0) = \int \delta\left(x_0 - x_T + \int_o^T f(T-t)h(t)\,\omega(t)dt\right)d\mu_\omega \tag{4}$$

employing the Fourier representation of the delta function (Bernido and Carpio-Bernido, 2015)

$$P(x_T, T; x_0, 0) = \frac{1}{2\pi}\int\int_{-\infty}^{+\infty} dk \exp(ik(x_0 - x_T))\exp\left(ik\int_o^T f(T-t)h(t)\,\omega(t)dt\right)d\mu_\omega \tag{5}$$

Now, we make use of the characteristic functional given by (Bernido & Carpio-Bernido, 2012)

$$C(\xi) = \int \exp\left(i\int_0^T \omega(t)\xi(t)dt\right)d\mu_\omega = \exp\left(-\frac{1}{2}\int_0^T \xi(t)^2\,dt\right) \tag{6}$$

Hence, the probability density function can be expressed as

$$P(x_T, T; x_0, 0) = \frac{1}{2\pi}\int_{-\infty}^{+\infty} dk\, exp(ik(x_0 - x_T))\, exp\left(-\frac{1}{2}k^2\int_o^T [f(T-t)h(t)]^2 dt\right) \tag{7}$$

Equation (7) is just a Gaussian integral and can be evaluated easily to get the final expression of the probability density as (Bernido and Carpio-Bernido, 2015)

$$P(x_T, T; x_0, 0) = \sqrt{\frac{1}{2\pi\left[\int_o^T f(T-t)h(t)\,dt\right]^2}}\exp\left[\frac{-(x_0 - x_T)^2}{2\int_o^T [f(T-t)h(t)]^2\,dt}\right].$$

The mean square displacement (MSD), which measures the deviation from the mean, can be calculated by

$$MSD = \langle (x - \langle x\rangle)^2\rangle = \langle x^2\rangle - \langle x\rangle^2 \tag{9}$$

To get the mean square displacement, one must be able to solve for the first moment and second moment: $\langle x\rangle$ and $\langle x^2\rangle$. To do this, we have to evaluate

$$\langle x\rangle = \int_{-\infty}^{+\infty} x\,P(x_T, T; x_0, 0)$$

and

$$\langle x^2\rangle = \int_{-\infty}^{+\infty} x^2\,P(x_T, T; x_0, 0).$$

The first moment with Equation (8) would lead us to a Gaussian integral that can be easily evaluated which gives $\langle x\rangle = x_0$. On the other hand, the second moment can be evaluated as (Bernido and Carpio-Bernido, 2015)

$$\langle x^2\rangle = \int_{-\infty}^{+\infty} x^2\,P(x_T, T; x_0, 0) = \sqrt{\frac{1}{2\pi\left[\int_o^T f(T-t)h(t)\,dt\right]^2}}\int x^2 \exp\left[\frac{-(x_0 - x_T)^2}{2\int_o^T [f(T-t)h(t)]^2\,dt}\right]dx$$

$$\langle x^2\rangle = x_0^2 + \int_o^T [f(T-t)h(t)]^2\,dt.$$

Thus, Equation (7) gives (Bernido and Carpio-Bernido, 2015)

$$MSD = \int_o^T [f(T-t)h(t)]^2\,dt \tag{10}$$

Equation (8) is now the general form of the mean square displacement of any system with a unique form of memory function $f(T-t)$ and $h(t)$.

Fractional Brownian Motion (fBM) and the MSD of Temperature Anomaly

Fractional Brownian motion have the following memory function (Bernido and Carpio-Bernido, 2015)

$$f(T-t) = \frac{(T-t)^{H-1/2}}{\Gamma(H+1/2)} \tag{11}$$

where $h(t) = 1$, and H is the Hurst exponent ($0<H<1$). The Hurst index can be attributed to normal diffusion or ordinary Brownian motion ($H = 1/2$), subdiffusion ($0 < H < 1/2$) or, superdiffusion ($1/2 < H < 1$) [1]. With this choice of the memory function, the probability density function in Equation (8) becomes

$$P(x_T, T; x_0, 0) = \sqrt{\frac{\Gamma^2\left(H+\frac{1}{2}\right)H}{\pi T^{2H}}}\exp\left[-\frac{H\Gamma^2\left(H+\frac{1}{2}\right)(x_0 - x_T)^2}{T^{2H}}\right]. \tag{12}$$

Using Equations (10) and (11), its mean square displacement can be obtained to yield (Bernido and Carpio-Bernido, 2015)

$$\mathbf{MSD} = \int_o^T [f(T-t)h(t)]^2\,dt = cT^\alpha, \tag{13}$$

where $\alpha = 2H$ and $c = \frac{1}{2H\Gamma^2\left(H+\frac{1}{2}\right)}$. Taking the logarithm of both sides of Equation (13), would arrive at a linear equation given by

$$\log(\text{MSD}) = \log c + \log(T^{2H}) = 2H\log(\text{T}) + \log c, \quad (14)$$

where the slope of this line is $2H$ and its intercept is log (c). Now, we can use Equation 12 with Hurst exponent $H = 1$, to fit the linear log-log plot of the MSD of temperature anomaly together with the 5-year moving average and the second-generation data of temperature anomaly shown in Figure 3. The result is shown in Figure 4.

As shown in Figure 4, both the treated and untreated data for temperature anomaly behaves linearly, almost having no difference at all. Aside from that, the three different data sets fit the fractional Brownian motion with Hurst exponent, $H = 1$. As mentioned previously, a Hurst exponent whose value can be found between 0.5 to 1.0 is attributed to superdiffusion. Most of the Brownian motion experiments and simulations in super diffusive regimes have been attributed to a force as given by the Langevin model (Despósito, 2011; Duplat et al., 2013). Using this idea to our case, the time-evolution of the temperature anomaly is driven by a *force* that can be traced back to anthropogenic effects on global warming and climate change. This is in agreement with (Vassoler et al., 2012) when they cited that most of the roots of global warming is caused by human activities, as well as, El Niño and La Niña, which are natural phenomena. Aside from that, (Enzler, 2013) cited that these human activities could warm the Earth by releasing carbon dioxide to the atmosphere. This is because increasing concentrations of atmospheric carbon dioxide resulted to increased infrared radiation absorption. Moreover, the Hurst exponent, *H*, being equal to 1 (boundary of the Hurst index in superdiffusion) can be attributed to the fact that the temperature anomaly data started 1880 and ended up to 2015. Human activities in relation to the warming of the Earth have high impact during this whole duration. In particular, the year 1880 happened to be following the so-called second Kondratiev wave, which began between about 1850 and 1870 (Bridgstock, 1998). This cycle of innovation in human history consisted mostly of the production of railways which swept across Europe and the United States. Furthermore, the first of such wave of innovations and technological change is the Industrial revolution itself during the latter part of eighteenth century. This cycle involves innovations in industries such as coal, iron and mining (Bridgstock, 1998).

a

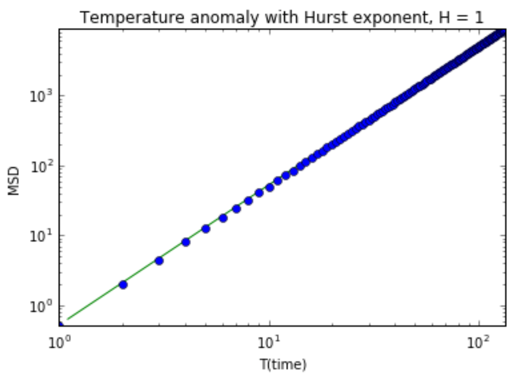

b

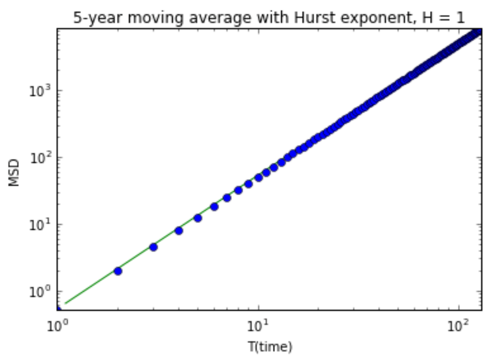

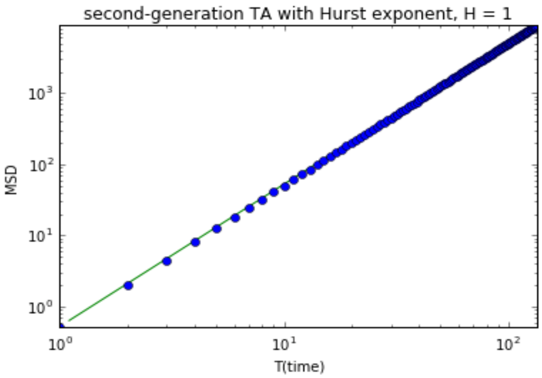

c

Figure 4. Mean Square displacement (MSD) of the (a) untreated Temperature Anomaly (TA), (b) 5-year moving average of TA and (c) second-generation temperature anomaly fitted with fractional Brownian motion (fBM) with Hurst exponent, $H = 1$.

CONCLUSION AND RECOMMENDATION

In this paper, the temperature anomaly data from year 1880-2015 has undergone two different data treatments: 5-year moving average and second-generation data. The second-generation data was obtained by subtracting the temperature anomaly data by the data points generated from a fit using polynomial of degree 4. Together with the untreated data, the log-log plot of mean square displacement (MSD) of temperature anomaly versus time was derived. The MSD, as shown in Figure 3, behaves linearly which could imply a fractional Brownian motion memory. Following the steps in white noise analysis (Bernido & Carpio-Bernido, 2012), the fractional Brownian motion memory function was used to derive its probability density function, as well as the MSD. Then, the logarithm of both sides of the obtained MSD was done to express it in linear form. The fBM with Hurst exponent, $H = 1$ was then used as a fit to the MSD of temperature anomaly which implies super-diffusion. Considering that global temperature follows a natural cycle when unperturbed, this anomalous behavior can be attributed to a driving *force* in the time evolution of the temperature anomaly. These 'forces' may be attributed to both the natural heating cycle in the Earth's surface and human activities particularly on technological changes and innovations which already begun even before the 1880s.

It is recommended that a more convincing statistical tool can be used in fitting of the MSD with the fractional Brownian motion with the Hurst exponent, e.g., *p*-value or chi-square.

REFERENCES

Bernido, C. C., & Carpio-Bernido, M. V. (2014). *Methods and Applications of White Noise Analysis in Interdisciplinary Sciences*. World Scientific.

Global Climate change, "Global temperatures as in indicator of global climate change", (2013). retrieved from: http://ete.cet.edu/gcc/?/global temp_teacherpage/

Enzler, S.M. "History of the Greenhouse Effect and global warming", Lenntech BV, (2013) retrieved from: http://www.lenntech.com /greenhouse-effect/global-warming-history.htm

Stock, C. A., Pegion, K., Vecchi, G. A., Alexander, M. A., Tommasi, D., Bond, N. A., ... & Xue, Y. (2015). Seasonal sea surface temperature anomaly prediction for coastal ecosystems. *Progress in Oceanography*, *137*, 219-236.

Hansen, J., Sato, M., Ruedy, R., Schmidt, G. A., Lo, K., & Persin, A. (2016). Global temperature in 2015. *GISS, NASA, NY. URL: http://data. giss. nasa. gov*.

Hansen, James, et al. (2010) "Global surface temperature change." *Reviews of Geophysics* 48.4.

GISTEMP Team. (2021). *GISS Surface Temperature Analysis (GISTEMP), version 4*. NASA Goddard Institute for Space Studies. Dataset accessed 2021-08-31 at https://data .giss.nasa.gov/gistemp/.

Lenssen, N., G. Schmidt, J. Hansen, M. Menne, A. Persin, R. Ruedy, & D. Zyss,(2019) . Improvements in the GISTEMP uncertainty model. *J. Geophys. Res. Atmos.*, 124, no. 12, 6307-6326, doi:10.1029/2018JD029522.

Bernido, C. C., & Carpio-Bernido, M. V. (2012). White noise analysis: some applications in complex systems, biophysics and quantum mechanics. *International Journal of Modern Physics B*, *26*(29), 1230014.

Despósito, M. A. (2011). Superdiffusion induced by a long-correlated external random force. *Physical Review E, 84*(6), 061114.

Duplat, J., Kheifets, S., Li, T., Raizen, M. G., & Villermaux, E. (2013). Superdiffusive trajectories in Brownian motion. *Physical Review E*, *87*(2), 020105.

Vassoler, R. T., & Zebende, G. F. (2012). DCCA cross-correlation coefficient apply in time series of air temperature and air relative humidity. *Physica A: Statistical Mechanics and its Applications*, *391*(7), 2438-2443.

Bridgstock, M., Burch, D., Forge, J., Laurent, J., & Lowe, I. (1998). *Science, technology and society: an introduction*. Cambridge University Press.